

INTERACTIONS OF LARGE SCALE STRUCTURES IN TURBULENT ROUND JETS

Jahnavi Kantharaju
DAAA, ONERA
92190 MEUDON France
jahnavi.kantharaju@onera.fr

Benjamin Leclaire
DAAA, ONERA
92190 MEUDON France
Benjamin.LECLAIRE@onera.fr

Laurent Jacquin
Fluid Mechanics and Energetic Branch , ONERA
Chemin de la Hunière - BP 801009
91123 PALAISEAU CEDEX - France
laurent.jacquin@onera.fr

ABSTRACT

The dynamical significance of vortical structures in the near field of round jets, viz. the vortex rings and the streamwise vortices, has been known for several decades (Ho & Huerre, 1984). A fundamental understanding of their interactions, especially in turbulent jets at high Reynolds number (Re), is expected to provide an impetus to devising control strategies; for instance in improving combustion efficiency and reducing jet noise. One such possible interaction was recently observed in Davoust *et al.* (2012) that involved production of additional streamwise vorticity, as a result of an influence of the fluctuations of streamwise vorticity on those of azimuthal vorticity in high Re jets. This additional vorticity showed up in streamwise vorticity correlations in the form of radial organization as opposed to its azimuthal organization classically found.

In further exploring this possibility, we have observed in our experiments, that strengthening the vortex rings relative to the streamwise vortices, renders them less susceptible to an influence from the streamwise vortices. This paper presents the results for a $Re = 1.5 \times 10^5$ and low Mach number round jet in which the most energetic vortex rings are acoustically excited at different excitation amplitudes. A comparison of the relative strengths of the two structures with increasing excitation levels, corroborates the interaction proposed in Davoust *et al.* (2012).

INTRODUCTION

The near field of a round jet is dominated by the axisymmetric mode ($m = 0$) in the form of vortex rings, streamwise vortices and small scale turbulence. The primary (Kelvin Helmholtz) instability of the free shear layer results in its rolling up into vortex rings. Whereas a three-dimensional instability of either the resulting vortex rings (Pierrehumbert & Widnall, 1982; Widnall & Sullivan, 1973) or the jet core itself (Lin & Corcos, 1984; Martin & Meiburg, 1991), gives rise to the secondary structures, streamwise vortices. The general organization of the flow in the near field, thus consists of a periodic array of the vortex rings and an azimuthal array of counter-rotating stream-

wise vortices (also referred to as ribs or braids), present in the region between the rings (called the "braid region"). Several studies have elucidated the existence and organization of these structures and their dynamical significance in jet mixing and entrainment (visualizations of Liepmann & Gharib (1992), vortex filament methods by Martin & Meiburg (1991) and simulations of Verzicco & Orlandi (1994) for instance).

The streamwise vortices have been observed to wrap around the rings (Bernal & Roshko, 1986), and influence them by distorting their cores (Verzicco & Orlandi, 1994; Comte *et al.*, 1998). Grinstein *et al.* (1996) exclusively studied such an interaction between vortex rings and externally generated streamwise vortices. They observed in their experiments that these interactions resulted in the deformation of the rings leading to their breakdown into small scale eddies. The co-existence of the vortex rings and the streamwise vortices indeed suggests the possibility of such an interaction between the two.

Recently in Davoust *et al.* (2012); Courtier (2014), interactions between fluctuating components of the azimuthal and streamwise vorticity was observed in a turbulent round jet, experimentally. Instead of the classical azimuthal array of counter-rotating streamwise vortices in the braid region, these vortices appeared to be organized in the radial direction. From a further analysis of the flow organization, the authors hypothesized that in high Re (Reynolds number based on diameter) jets, a scenario based on vortex induction mechanisms as shown in figure 1, can be possible. It was attributed to their finding that the fluctuations of azimuthal vorticity (corresponding to $m = 0$ mode) were weaker than that of the streamwise component. Considering the vorticity fluctuations, it basically involves an interaction between a periodic array of vortex rings and a strong streamwise vortex located between two positive azimuthal vorticity. (The alternating sign of azimuthal vorticity arises due to the fluctuating field). The streamwise vorticity tends to deform the negative azimuthal vorticity in the radial direction. These deformations are further reoriented in the axial direction by the mean shear resulting in the formation of streamwise vorticity of the opposite sign in the radial di-

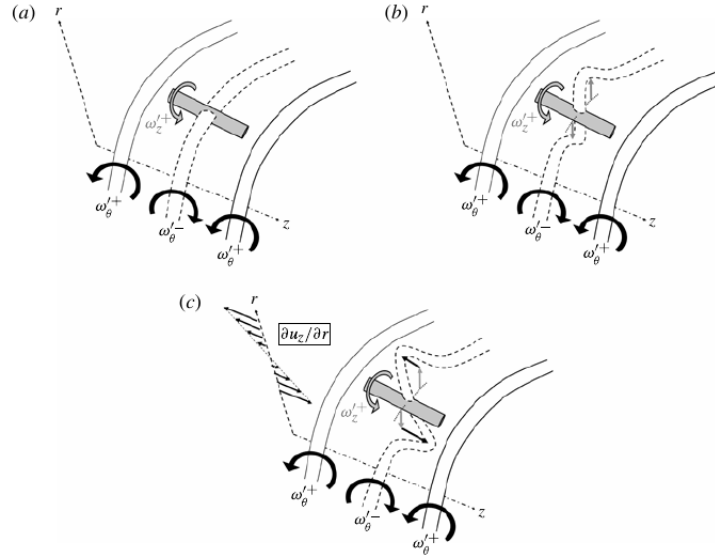


Figure 1: Proposed scenario in Davoust *et al.* (2012) that considers an interaction between the fluctuations of azimuthal and streamwise vorticity in a turbulent round jet at $Re = 2.1 \times 10^5$ a) The considered initial location of a streamwise vortex with respect to the axisymmetric mode. b) Deformation of the negative azimuthal vorticity fluctuation by the streamwise vortex. c) Reorientation of the deformed part by mean shear.

rection.

These observations motivated us to further explore and confirm the possibility of such an interaction, and its dependence on Re . We varied the relative strengths of the vorticity fluctuations by acoustically exciting the vortex rings. We observed that the radial array of streamwise vortices in the unexcited jet, shifted towards an azimuthal configuration which is found at lower Re , with increasing levels of excitation. This paper presents the results for a $Re = 1.5 \times 10^5$ jet that is axisymmetrically excited and discusses the influence of streamwise vortices on the vortex rings in a cross sectional plane two diameters downstream of the nozzle.

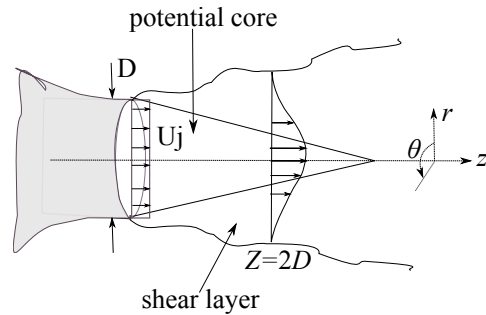


Figure 2: Definition of the round jet studied.

METHOD

A round air jet exiting from a nozzle of 15 cm diameter (D) with a velocity, $U_j = 15.8$ m/s as shown in figure 2 is generated in an open-circuit wind tunnel, R4 at ONERA Meudon and is studied using High Speed Stereo Particle Image Velocimetry (HS-SPIV) and hot wire anemometry (HWA). HS-SPIV is performed in a cross sectional plane two diameters downstream of the nozzle exit ($Z = 2D$). The exiting boundary layer is transitional and the mean velocity has a top-hat profile.

Experiments

For the HS-SPIV, two Phantom V710 high speed cameras equipped with 105 mm lenses at an $f_{\#} = 8$ aperture have been used in forward scattering configuration. A high repetition rate double pulse Nd-YLF 527 nm laser synchronized with the cameras generates a 2.5 mm thick light sheet. The inter-pulse time is adjusted such that a maximum displacement of 7 pixels is obtained on the camera CCDs. Sixteen blocks of 4096 double frame image pairs are recorded at an acquisition frequency, $F_a = 2.5$ kHz. Velocity vectors are computed from the particle image pairs using FOLKI-SPIV, an in-house post-processing tool detailed in Cham-

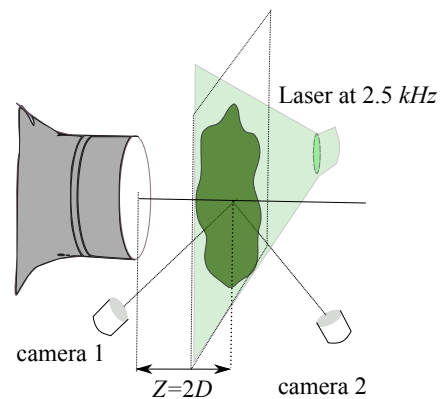


Figure 3: HS-SPIV setup: the measurement plane is at $z = 2$ capturing the entire jet.

pagnat *et al.* (2011). An interrogation window (IW) size of 31 pixels was chosen which yielded a spatial resolution of the vector field of 5.4 mm in the object plane.

The acoustic excitation is employed by means of a loudspeaker mounted on top of the settling chamber that provides axisymmetric forcing at the nozzle exit. The loud-

speaker is driven by a pure sine wave whose amplitude can be varied through the root mean square of the voltage supplied to the loudspeaker. The excitation frequency was fixed at the resonant frequency of the settling chamber (52 Hz) that yielded significant excitation amplitudes at the nozzle exit. This corresponded to a non dimensional $f = 0.49$.

Post-processing

We used Spectral Proper Orthogonal Decomposition (SPOD) to extract the most energetic structures in the flow, as has been applied by Citriniti & George (2000) for instance, to round jets. Briefly explained, it seeks an optimal basis for a given ensemble of velocity snapshots maximizing the amount of kinetic energy contained. Due to statistical stationarity and azimuthal homogeneity of the flow, the SPOD eigenfunctions in time and azimuthal direction are then the Fourier modes. Hence, each component (u_i for $i = z, r, \theta$) of the velocity fluctuations were first Fourier transformed in t and θ as

$$\hat{u}_i(r, m, f) = \int_0^{t_0} \int_0^{2\pi} u'_i(r, \theta, t) e^{-i(m\theta + 2\pi ft)} d\theta dt \quad (1)$$

where t_0 is the acquisition length of each block. POD modes $\phi_i^{(n)}(r, m, f)$ with $n = 1, 2, \dots$, for the given ensemble are found using

$$\int_0^{r_0} B_{ij}(r, r', m, f) \phi_j^{(n)}(r', m, f) dr' = \lambda^{(n)}(m, f) \phi_i^{(n)}(r, m, f) \quad (2)$$

where r_0 is the radial extent of the flow. The Hermitian symmetric kernel (B_{ij}) is the weighted two point cross-spectrum given by

$$B_{ij}(r, r', m, f) = r^{1/2} \langle \hat{u}_i(r, m, f) \hat{u}_j^*(r', m, f) \rangle r'^{1/2} \quad (3)$$

with x^* representing the complex conjugate of x . $\langle \rangle$ denotes the ensemble average over all the data blocks. The members of the ensemble can be reconstructed through

$$\hat{u}_i(r, m, f) = \frac{1}{r^{1/2}} \sum_n \hat{a}^{(n)}(m, f) \phi_i^{(n)}(r, m, f) \quad (4)$$

where $\hat{a}^{(n)}(m, f)$ are the random coefficients found by projecting the velocity vector onto the POD basis as:

$$\hat{a}^{(n)}(m, f) = \int_0^{r_0} r^{1/2} \hat{u}_i(r, m, f) \phi_i^{*(n)}(r, m, f) dr \quad (5)$$

An algorithm similar to Towne *et al.* (2018) was implemented to compute the POD basis with 256 blocks and 512 samples per block yielding a frequency resolution of 4.8 Hz ($f \approx 0.03$). For the unexcited jet, the $n = 1$ POD mode contained about 58% of the total kinetic energy while it was as high as 90% in the most excited case ($u_z^{rms}|_{z=0} = 4.8\%$).

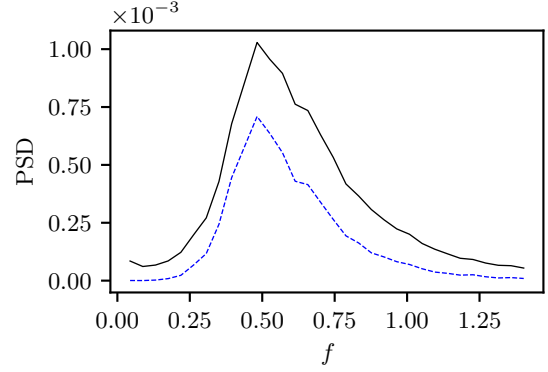


Figure 4: Power spectral density of the axial velocity for the unforced jet with (—) corresponding to the full spectra and (- - -) to the contribution from the ($n = 1$, $m = 0$) SPOD mode.

RESULTS AND DISCUSSION

In the following sections, the upper-case (R, θ, Z) and lower-case (r, θ, z) symbols represent dimensional and non-dimensional quantities in the cylindrical coordinate system. Since we are studying the jet dynamics at two diameter downstream of the nozzle, the diameter is found to be a more appropriate length scale compared to the shear layer momentum thickness. Length and velocity scales used for non-dimensionalization are the nozzle exit diameter (D) and jet velocity (U_j) respectively. Time and frequency are expressed in non-dimensional forms as well, with t and f respectively, with the latter being the Strouhal number given by $f = FD/U_j$. We denote the components of the mean velocity by u_r, u_θ, u_z , the fluctuations by a prime and the turbulence intensities by *rms* in the superscript (i.e. $u_z^{rms} = \langle u_z'^2 \rangle^{1/2}$).

On the frequency and amplitude of excitation

First, the frequency and amplitude of excitation were determined. To increase the strength of the rings, we excited the most energetic axisymmetric mode. This was found from the contribution of the first SPOD ($n=1$) mode to the kinetic energy spectra of the axial velocity, corresponding to $m = 0$ in the jet core at $r = 0.24$ as shown in figure 4. It can be seen that the $m=0$ mode is dominant over a range of frequencies, a characteristic of noise amplifiers. The results for excitation at the frequency of the local peak in the spectra i.e. $f = 0.49$ are discussed in this paper.

The excitation amplitude is characterized in terms of turbulence intensities at the nozzle exit ($u_z^{rms}|_{z=0}$) along the centerline, following the work of Crow & Champagne (1971). The response of the jet at $z = 2$, the HS-SPIV measurement plane, at $f = 0.49$ is displayed in figure 5. As observed in Crow & Champagne (1971), the near field of a jet acts as a non-linear oscillator amplifying the input disturbances. There is an almost linear amplification at low excitation levels, which tends to saturate to a maximum value of turbulence intensity of 11% at $z = 2$. This saturation can be attributed to the growth of the first harmonic with the increase in the amplitude of excitation.

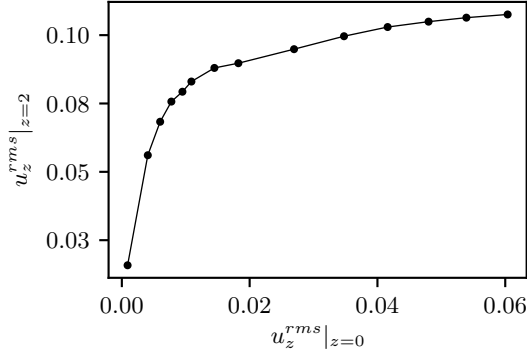


Figure 5: Response of the jet at $z = 2$ in terms of turbulence intensities at the nozzle exit ($z = 0$) along the centerline of the jet.

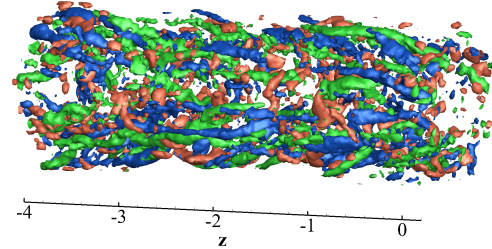
Taylor's reconstruction

Since in our experiments, the HS-SPIV measurement plane is at a fixed cross section, the local spatial structure of the flow in the axial direction is derived from the temporal snapshots using Taylor's hypothesis. For low turbulence intensities compared to the mean flow speed, Taylor's hypothesis of frozen turbulence allows one to view temporal fluctuations at a fixed point in space as a result of a frozen spatial structure convecting past that point at the mean flow speed (or the convection velocity U_c). An appropriate convection velocity and the validity of the hypothesis must be carefully considered while applying this hypothesis. Davoust & Jacquin (2011) have found the convection velocity of $U_c = 0.6U_j$ to be appropriate for a similar jet in the frequency range we are interested in this study and that the Taylor's approximation holds satisfactorily until $r = 0.7$.

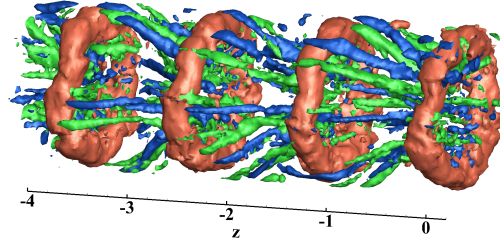
We can derive a physical intuition for the flow and the effect of excitation through such a reconstruction shown in figure 6 for a natural jet and its excited counterpart at excitation level of $u_z^{rms}|_{z=0} = 4.8\%$. The axial coordinate is $z = -u_c t$. As expected, excitation is seen to raise the inherent order of turbulent flow above the background noise. Also, in the excited case one can discern the classical structure of the near field of a jet through excitation, that consists of a periodic array of vortex rings and counter-rotating streamwise vortices, organized in the azimuthal direction. The wrapping of the streamwise vortices around the rings is evident in the excited jet. Also, the inclination of the streamwise vortices towards the jet centerline near the upstream region of the rings, while away from the centerline immediately downstream can be observed. Whereas in the unexcited jet, they tend to be more aligned in the axial direction.

Streamwise vorticity organization

Next, we look at how streamwise vorticity is organized in a statistical sense in the cross sectional plane. Two point correlations help in this regard to understand the structure of a turbulent flow as was demonstrated for instance in Rogers & Moin (1987). In order to visualize the ω_z organization in our flow, we compute the following auto-correlation of the streamwise vorticity fluctuations (Davoust *et al.*, 2012):



(a)



(b)

Figure 6: Taylor's reconstruction of vorticity fluctuations in the axial direction ($z = -u_c t$) for a) the natural jet b) the excited jet at $u_z^{rms}|_{z=0} = 4.8\%$. The orange contours correspond to iso-surfaces of $\omega'_\theta = +5$, the green and blue to that of $\omega'_z = +3$ and $\omega'_z = -3$ respectively. The flow is from left to right.

$$C_{\omega_z \omega_z}(r, r', \theta', t') = \frac{\langle \omega'_z(r, \theta, t) \omega'_z(r', \theta + \theta', t + t') \rangle_\theta}{\langle \omega_z'^2(r, \theta, t) \rangle_\theta^{1/2} \langle \omega_z'^2(r', \theta, t) \rangle_\theta^{1/2}} \quad (6)$$

where $\langle \cdot \rangle_\theta$ denotes average over data blocks and θ as the flow has statistical stationarity and azimuthal homogeneity.

Contours of $C_{\omega_z \omega_z}$ for $t' = 0$ i.e. correlation of ω_z at a particular instant of time in the cross-section averaged over all snapshots would give a probable vortex structure in a statistical sense. Figure 7 shows a typical organization for the radial and azimuthal arrays of streamwise vortices on the top and bottom respectively.

The streamwise vorticity correlations were checked for different excitation levels with reference to figure 5, out of which four cases were studied in detail, viz. the unexcited jet and excitation at three amplitudes $u_z^{rms}|_{z=0} = 1.4\%$, 2.6% and 4.8% . These were chosen based on the observed organization of the streamwise vortices, such that the cases represented each type of organization. The unexcited jet contained radial arrays and with the increasing excitation levels, the radial organization started to disappear. Hence the term transitional for $u_z^{rms}|_{z=0} = 1.4\%$ where the organization was somewhat intermediate between the two configurations. Around $u_z^{rms}|_{z=0} = 2.6\%$, a complete switch to azimuthal configuration was observed. The excitation level was further increased to $u_z^{rms}|_{z=0} = 4.8\%$ to determine the effect of very high excitation levels.

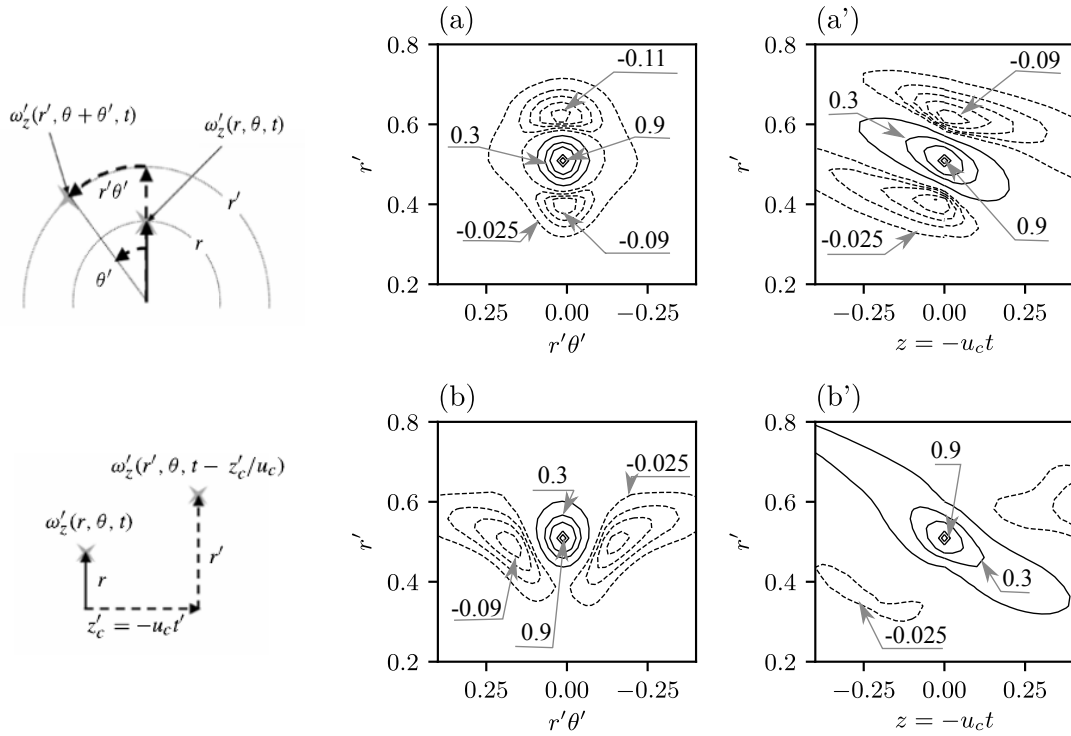


Figure 7: A typical organization of streamwise vorticity at the center of the shear layer, $r/D = 0.5$: Iso-contours of $C_{\omega_z \omega_z}(r = 0.5, r', \theta', t' = 0)$ for the jet (a) without excitation (radial) (b) excitation at $St_D = 0.49$, $u_z^{rms}|_{z=0} = 2.6\%$ (azimuthal) at $z = 2$. (a', b') are in a longitudinal plane locally reconstructed using Taylor's hypothesis around $z = 2$. On the extreme left, a schematic to evaluate the correlation, in the cross sectional plane on the top and in the longitudinal plane at the bottom, is shown (Davoust *et al.*, 2012). Solid lines (—) represent positive correlation while dashed lines (- -) represent negative correlation.

Effect of excitation

We then, looked at the changes in the radial distribution of velocity and vorticity components as the jet is excited to further characterize the axisymmetric excitation.

The radial profiles of turbulence intensities at $z = 2$ revealed an increase in the axial and radial components of velocity, which are mainly induced by the vortex rings, with no appreciable change in the azimuthal component. Figure 8a shows the radial profile of the u_z^{rms} where the profile develops a local minima near the core of the vortex ring. This could be due to the regularization in the formation of vortex rings at the excitation frequency.

It can be seen from figure 8b that ω_z^{rms} remains almost the same with increasing levels of excitation. This suggests that the scale of the streamwise vortices does not change with excitation except that the profile develops two maxima for the most excited case. The location of the maxima is at radial positions where the streamwise vortices are closest to the rings as can be seen in figure 6.

Comparison of strengths

Having observed a transition in the streamwise vorticity organization with increasing excitation levels, we sought a quantitative estimate for the strengths of the fluctuations, to evaluate the possibility of a ring deformation by the streamwise vortices. The scale of streamwise vortices was estimated from the maximum of ω_z^{rms} in the shear layer. Whereas for the rings, their strengths can be estimated from the *rms* of azimuthal vorticity fluctuations reconstructed

from ($n = 1, m = 0$) SPOD mode at $r = 0.5$.

This comparison of strengths along with the observed vorticity organization is given in table 1. It can be seen that as the excitation level is increased, the scale of the fluctuations of azimuthal vorticity increases with respect to those of streamwise vorticity. This can also be interpreted as the vortex rings getting stronger with the excitation level. At the highest level of excitation, they are of comparable strengths. Along with which, a corresponding shift in the organization of streamwise vortices towards the azimuthal array is found.

Our assumption that the observed radial organization at high *Re* unexcited jets, could stem from a mechanism conjectured in Davoust *et al.* (2012) (as described in our introduction section) is thus validated. Indeed, an interaction between the fluctuations of azimuthal and streamwise vorticity together with a contribution from the mean shear can result in organized radial arrays of streamwise vortices.

CONCLUSION

Interactions between large scale structures in turbulent flows can play an important role in producing smaller eddies, and in transition to turbulence. One such possible interaction between the fluctuations of streamwise and azimuthal vorticity in the near field of a high *Re* round jet was investigated in this work. We observed that as the rings (azimuthal vorticity fluctuations) are excited, the radial array of streamwise vortices found in the unexcited jet, shifted towards an azimuthal configuration which has been reported for lower *Re* jets in the cited literature. In the unexcited

jet, as the vortex rings were found to be weak compared to streamwise vortices, the rings could undergo a deformation by the latter. By acting on the strength of the rings through acoustic excitation, we have shown that such an interaction, is indeed possible.

Next step is to further characterize this interaction and study its effect on the near field entrainment. Conditional sampling is being employed to analyze the flow in the ring and the braid regions, and compare with the visualizations available in the literature at lower Re . Effect of Re and excitation parameters will also be assessed. The long term goal of this study is to develop a theoretical model to describe these interactions.

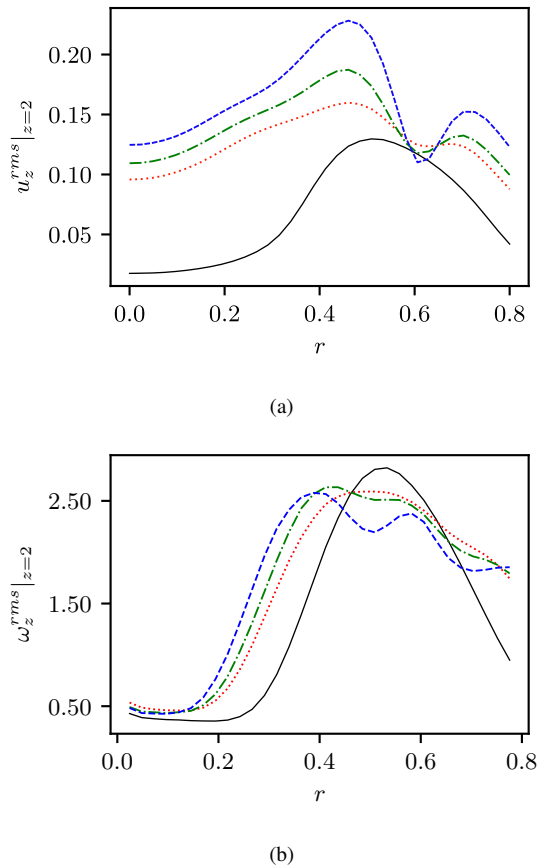


Figure 8: Radial profiles of rms of a) axial velocity b) streamwise vorticity at $z = 2$; where, solid line (—) represents the unexcited jet, (...) excitation at $u_z^{rms} = 1.4\%$, (-.-) at 2.6% and (- - -) at 4.8%

Table 1: Variation of the relative strengths through excitation and the corresponding streamwise vorticity organization

case	$u_z^{rms} _{z=0}$	ω'_θ/ω'_z	organization type
1Unforced	-	0.16	radial
2forced	1.4 %	0.68	transitional
3forced	2.6 %	0.83	azimuthal
4forced	4.8 %	1.05	azimuthal

REFERENCES

- Bernal, LP & Roshko, Alan 1986 Streamwise vortex structure in plane mixing layers. *Journal of Fluid Mechanics* **170**, 499–525.
- Champagnat, Frédéric, Plyer, Aurélien, Le Besnerais, Guy, Leclaire, Benjamin, Davoust, Samuel & Le Sant, Yves 2011 Fast and accurate piv computation using highly parallel iterative correlation maximization. *Experiments in fluids* **50** (4), 1169.
- Citriniti, JH & George, William K 2000 Reconstruction of the global velocity field in the axisymmetric mixing layer utilizing the proper orthogonal decomposition. *Journal of Fluid Mechanics* **418**, 137–166.
- Comte, P, Silvestrini, JH & Bégou, P 1998 Streamwise vortices in large-eddy simulations of mixing layers. *European Journal of Mechanics-B/Fluids* **17** (4), 615–637.
- Courtier, Romain 2014 Influence of initial conditions on dynamics of large scales in turbulent jets. PhD thesis.
- Crow, S Cj & Champagne, FH 1971 Orderly structure in jet turbulence. *Journal of Fluid Mechanics* **48** (03), 547–591.
- Davoust, S & Jacquin, L 2011 Taylor’s hypothesis convection velocities from mass conservation equation. *Physics of Fluids* **23** (5), 051701.
- Davoust, S, Jacquin, L & Leclaire, B 2012 Dynamics of $m=0$ and $m=1$ modes and of streamwise vortices in a turbulent axisymmetric mixing layer. *Journal of Fluid Mechanics* **709**, 408–444.
- Grinstein, FF, Gutmark, EJ, Parr, TP, Hanson-Parr, DM & Obeysekare, U 1996 Streamwise and spanwise vortex interaction in an axisymmetric jet. a computational and experimental study. *Physics of Fluids* **8** (6), 1515–1524.
- Ho, Chih-Ming & Huerre, Patrick 1984 Perturbed free shear layers. *Annual Review of Fluid Mechanics* **16** (1), 365–422.
- Liepmann, Dorian & Gharib, Morteza 1992 The role of streamwise vorticity in the near-field entrainment of round jets. *Journal of Fluid Mechanics* **245**, 643–668.
- Lin, S cJ & Corcos, GM 1984 The mixing layer: deterministic models of a turbulent flow. part 3. the effect of plane strain on the dynamics of streamwise vortices. *Journal of Fluid Mechanics* **141**, 139–178.
- Martin, J. E. & Meiburg, E. 1991 Numerical investigation of three-dimensionally evolving jets subject to axisymmetric and azimuthal perturbations. *Journal of Fluid Mechanics* **230**, 271–318.
- Pierrehumbert, RT & Widnall, SE 1982 The two-and three-dimensional instabilities of a spatially periodic shear layer. *Journal of Fluid Mechanics* **114**, 59–82.
- Rogers, Michael M & Moin, Parviz 1987 The structure of the vorticity field in homogeneous turbulent flows. *Journal of Fluid Mechanics* **176**, 33–66.
- Towne, Aaron, Schmidt, Oliver T & Colonius, Tim 2018 Spectral proper orthogonal decomposition and its relationship to dynamic mode decomposition and resolvent analysis. *Journal of Fluid Mechanics* **847**, 821–867.
- Verzicco, R & Orlandi, P 1994 Direct simulations of the transitional regime of a circular jet. *Physics of Fluids* **6** (2), 751–759.
- Widnall, Sheila E & Sullivan, JP 1973 On the stability of vortex rings. *Proc. R. Soc. Lond. A* **332** (1590), 335–353.